Molecular Therapy
Nucleic Acids
Original Article

Morpholino Antisense Oligomers as a Potential Therapeutic Option for the Correction of Alternative Splicing in PMD, SPG2, and HEMS

Stephanie Tantzer,[1] Karen Sperle,[1] Kaitlin Kenaley,[1,2] Jennifer Taube,[1] and Grace M. Hobson[1,3,4]

[1]Nemours Biomedical Research, Alfred I. duPont Hospital for Children, Wilmington, DE 19803, USA; [2]Department of Pediatrics/Neonatology, Christiana Care Health System, Newark, DE 19713, USA; [3]Department of Biological Sciences, University of Delaware, Newark, DE 19716, USA; [4]Department of Pediatrics, Jefferson Medical College, Thomas Jefferson University, Philadelphia, PA 19107, USA

DNA variants of the proteolipid protein 1 gene (*PLP1*) that shift *PLP1/DM20* alternative splicing away from the *PLP1* form toward *DM20* cause the allelic X-linked leukodystrophies Pelizaeus-Merzbacher disease (PMD), spastic paraplegia 2 (SPG2), and hypomyelination of early myelinating structures (HEMS). We designed a morpholino oligomer (MO-PLP) to block use of the *DM20* 5′ splice donor site, thereby shifting alternative splicing toward the *PLP1* 5′ splice site. Treatment of an immature oligodendrocyte cell line with MO-PLP significantly shifted alternative splicing toward *PLP1* expression from the endogenous gene and from transfected human minigene splicing constructs harboring patient variants known to reduce the amount of the *PLP1* spliced product. Additionally, a single intracerebroventricular injection of MO-PLP into the brains of neonatal mice, carrying a deletion of an intronic splicing enhancer identified in a PMD patient that reduces the *Plp1* spliced form, corrected alternative splicing at both RNA and protein levels in the CNS. The effect lasted to post-natal day 90, well beyond the early post-natal spike in myelination and PLP production. Further, the single injection produced a sustained reduction of inflammatory markers in the brains of the mice. Our results suggest that morpholino oligomers have therapeutic potential for the treatment of PMD, SPG2, and HEMS.

INTRODUCTION

Aberrant alternative splicing is a frequent cause of human disease.[1,2] An estimated 70% of human multi-exon genes are subject to alternative splicing, a process that allows genes to code for multiple proteins, thereby increasing protein diversity of the genome.[3,4] The process of alternative splicing is generally tightly regulated by sequence elements in pre-mRNA that act as enhancers or silencers and bind protein-splicing factors or form secondary structures that influence splice site selection.[5–9] The interplay of these elements and factors along with the general splicing elements and binding factors at 5′ splice donor sites, 3′ acceptor sites, and branch points results in inclusion or exclusion of whole exons or parts of exons in the mRNA.[2] Disease can result when a splicing enhancer or silencer is weakened, strengthened, or destroyed by mutation.[2]

The proteolipid protein 1 gene (*PLP1*; MIM: 300401) encodes proteolipid protein (PLP), a four-pass transmembrane protein that is the major protein of myelin in the CNS. Human and mouse *PLP1* have two major splice isoforms due to alternative use of splice donor sites, one at the 3′ end of exon 3A and the other 105 bases downstream at the 3′ end of exon 3B, resulting in the mRNA transcripts *DM20* and *PLP1*, respectively (Figure 1A).[10] The DM20 protein produced from the splice donor site at the 3′ end of exon 3A is internally deleted for 35 amino acids of the first intracellular loop with respect to PLP produced from the donor site at exon 3B. A developmental switch occurs in the isoform ratio from DM20 as the predominant form during embryogenesis to PLP as the predominant form during and after active myelination, when there is a dramatic upregulation of *PLP1* gene expression.[11–13]

We and others have shown that aberrant alternative splicing of *PLP1*, due to DNA variants in the 5′ splice donor sites or in splicing enhancer elements, causes the allelic X-linked leukodystrophies Pelizaeus-Merzbacher disease (PMD; OMIM: 312080) or the milder spastic paraplegia 2 (SPG2; OMIM: 312920), indicating that stringent regulation of the *PLP1/DM20* alternative splice is of critical importance for normal CNS function.[8,14–29] Recently, hypomyelination of early myelinating structures (HEMS), which is allelic but distinguished from PMD and SPG2 by the early hypomyelination seen on MRI, was also shown to be caused by misregulation of alternative splicing of *PLP1*.[30] Clinical signs of PMD, SPG2, and HEMS include nystagmus and hypotonia that progresses to spasticity.[30–32]

Amino acid changes in PLP have been shown to cause protein misfolding, accumulation in the endoplasmic reticulum (ER), and ER stress leading to disease,[33–35] but alternative splicing variants do not necessarily cause amino acid changes. Abnormal alternative splicing alone, even with the absence of an amino acid change, causes

Received 22 May 2018; accepted 22 May 2018;
https://doi.org/10.1016/j.omtn.2018.05.019.

Correspondence: Grace M. Hobson, PhD, Nemours Biomedical Research, Alfred I. duPont Hospital for Children, 1600 Rockland Road, Wilmington, DE 19803, USA.
E-mail: ghobson@nemours.org

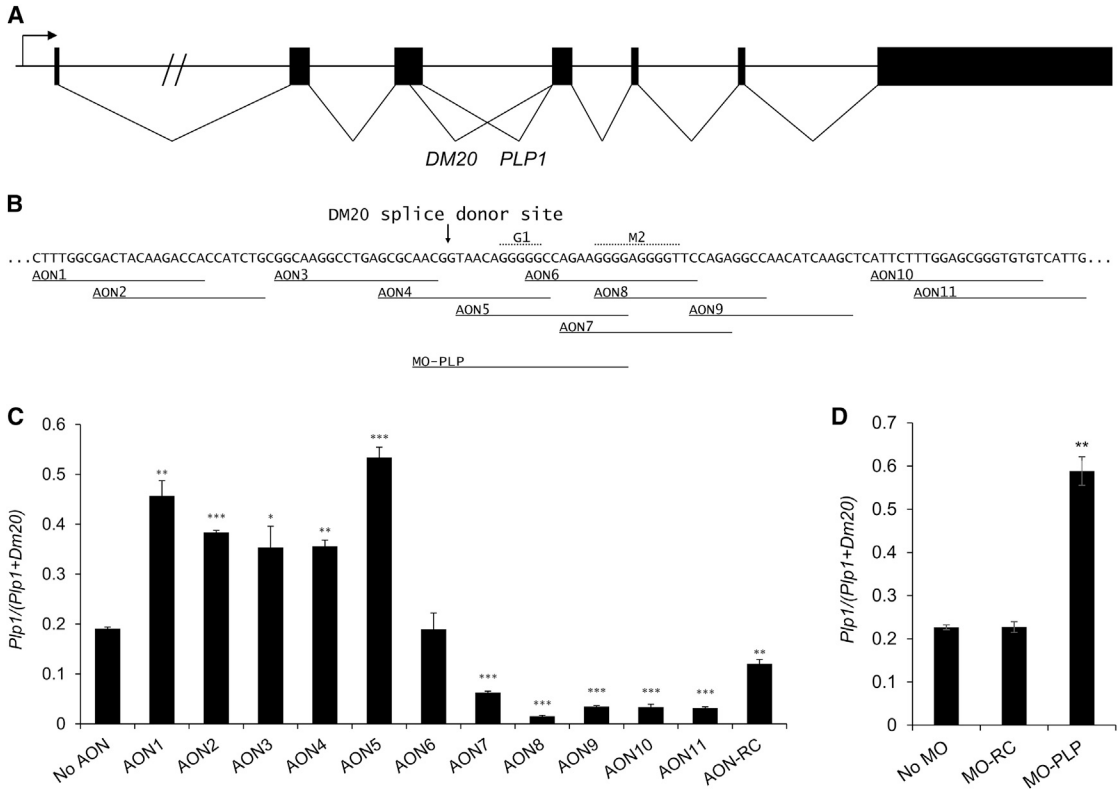

Figure 1. Modification of Alternative Splicing of *Plp1* Using AONs and MO-PLP

(A) Diagram of *Plp1* showing the *Plp1/Dm20* alternative splice. Structures of the human and mouse genes are alike. (B) DNA sequence across the *Dm20* splice donor site showing locations covered by AONs and MO-PLP used to treat Oli-neu cells. (C and D) RT-PCR analysis was performed to determine the effect of treating Oli-neu cells with (C) the series of AONs or (D) MO-PLP on endogenous expression levels of the *Plp1* and *Dm20* alternatively spliced products. Treatments were performed in triplicate cell cultures. Data are shown as mean ± SD; p values are for treated samples compared to the untreated sample, *$p < 0.05$, **$p < 0.01$, and ***$p < 0.001$. AONs that bind upstream of and including the *Dm20* splice donor site increased the endogenous *Plp1* alternatively spliced product, while those downstream, except for AON6, decreased it. MO-PLP significantly increased the endogenous *Plp1* alternatively spliced product in Oli-neu cells. The capillary electrophoresis data for (C) and (D) are shown in Tables S1 and S2, respectively. MO-PLP dose response for the modification of alternative splicing in Oli-neu cells and visual representation of the data are shown in Figure S1.

disease.[8,30] However, there are some variants that cause both abnormal alternative splicing and an amino acid change, and, in that case, ER stress likely contributes to the disease in the patient. The alternative splicing variants are also not copy number variants like the PLP nulls and more common duplications that result in no PLP protein or presumably overexpression, respectively.[36,37] Rather, they shift the relative amounts of the PLP and DM20 isoforms while maintaining a normal amount of total protein.[8] It is not known how these alternative splicing variants cause disease, but shifting the relative amounts of PLP and DM20 isoforms toward normal seems to be a viable therapeutic approach.

There are currently no therapeutic interventions for PMD, SPG2, and HEMS. However, molecules that modulate alternatively spliced products are being developed and tested as therapeutic interventions for several diseases caused by the disruption of alternative splicing.[38–40] Antisense oligomers are among the most promising strategies. In one study, a morpholino antisense oligomer shifted the aberrant *PLP1*/*DM20* alternative splicing produced by a patient with PMD, due to a variant in exon 3B that reduces the *PLP*-specific form, toward normal in cultured oligodendrocyte precursor cells.[41] In this case, the antisense oligomer used was specific for that particular patient's variant.

Currently, the most successful antisense therapy approach for the correction of a splicing defect has been for spinal muscular atrophy, type I (SMA1; OMIM: 253300).[42,43] SMA1 is caused by the underproduction of survival of motor neuron protein (SMN) produced from the *SMN1* gene (SMN1; OMIM: 600354). A second gene, *SMN2* (OMIM: 601627), produces the identical protein to *SMN1*, but much less of it because of an intronic variant that leads to a high level of skipping of exon 7 and the formation of a nonfunctional protein that is degraded. In approaches for the treatment of SMA, antisense oligomers are made to target intronic splicing regulatory elements in *SMN2* to dramatically increase exon inclusion, overcoming the effect of the variant in *SMN2* and leading to the production of more normal levels of SMN protein. In preclinical testing of this approach by the introduction of antisense molecules into the CNS of SMA mice,

symptoms of severe SMA were ameliorated.[44,45] In clinical trials by Ionis Pharmaceuticals (formerly ISIS Pharmaceuticals), the antisense therapy proved to be safe and well-tolerated in a phase 1 trial[46,47] and to have encouraging clinical efficacy in a phase 2 trial, showing improved motor function and ventilation-free survival in infantile-onset SMA patients, and FDA approval has been granted.[48] A phase 3 trial is still underway.

In this study, we demonstrate that antisense RNA and morpholino oligomers designed to target variants in splice regulatory elements in *PLP1* exon 3 can cause switching of alternative *PLP1/DM20* splicing in cell culture. Further, when administered via intracerebroventricular injection in a mouse model with aberrant alternative splicing, a morpholino oligomer designed to target the *DM20* splice donor site can normalize levels of products by shifting alternative splicing toward the *PLP1* form in the CNS, reducing markers of brain inflammation. Therefore, we suggest antisense oligomers may be a therapeutic option for the treatment of patients with PMD, SPG2, and HEMS who have variants that affect alternative splicing.

RESULTS

Antisense Oligonucleotides Affect Levels of Endogenous PLP1 and DM20 Alternatively Spliced Products in Oli-neu Cells

We have shown that some pathogenic variants of the *PLP1* gene decrease the *PLP1* alternatively spliced form without changing the coding sequence of either product, so normalizing alternatively spliced levels of *PLP1* and *DM20* might be a therapeutic option for patients with these variants. In addition, variants in exon 3B that do change the coding sequence and also cause an alternative splicing error sometimes result in more severe disease than variants that only change the coding sequence, so normalizing levels of alternatively spliced products might be a therapeutic option for these patients as well.[41] To determine sequences that would be the best targets for influencing *Plp1* and *Dm20* alternative splicing, we treated mouse Oli-neu cells with a series of antisense oligonucleotides (AONs) designed to bind the *Dm20* splice site and surrounding region of the endogenous *Plp1* gene and, thereby, alter the levels of *Plp1* and *Dm20* splice products.[49] The Oli-neu cell line, an immortalized oligodendrocyte precursor cell line, was chosen because it inherently expresses mostly *Dm20* with low levels of *Plp1*, allowing easy detection of a shift in the alternatively spliced products toward *Plp1*.[50] We reasoned that AONs could block *Dm20* splicing either directly by binding to the *Dm20* 5′ splice donor site or indirectly by binding to regions that contain splice regulatory factors, thereby shifting the splicing toward more of the *Plp1* form.

We designed 11 2′-O-methyl RNA AONs, designated AON1–AON11, to bind within *Plp1* exon 3 (Figure 1B). AON4 targets the *Dm20* 5′ splice site. AON5–AON8 target the G1 and M2 sequences that have been shown to play a role in the regulation of *DM20* splice site selection.[51–53] The remaining AONs target other nearby potential regulatory sequences.[51,52] A random sequence was used as a negative control, AON-RC. Each AON was individually transfected into Oli-neu cells, and RT-PCR analysis was performed to determine the relative levels of endogenous *Plp1* and *Dm20*; the results are shown (Figure 1C; Table S1). Approximately 20% of the total signal from the *Plp1* gene (*Plp1* + *Dm20*) in untreated Oli-neu cells was *Plp1*. One AON, AON6, had no effect on *Plp1/Dm20* alternative splicing, while five increased and five decreased the amount of *Plp1* in total *Plp1* + *Dm20* product. Five AONs that bound in exon 3B downstream of the *Dm20* 5′ splice site (AON7, AON8, AON9, AON10, and AON11) all significantly decreased the amount of *Plp1* in the total product (3.1-fold, 12.7-fold, 5.6-fold, 5.6-fold, and 6.0-fold compared to no treatment, respectively). Those that bound at the *Dm20* 5′ splice site or upstream in exon 3A (AON1, AON2, AON3, AON4, and AON5) all significantly increased *Plp1* in the total product (2.4-fold, 2.0-fold, 1.9-fold, 1.9-fold, and 2.8-fold compared to no treatment, respectively). These data demonstrate the complexity of the sequences within exons 3A and 3B that regulate *Plp1/Dm20* alternative splicing. The random control AON-RC decreased the *Plp1* in the total product 1.6-fold compared to no treatment. This unexpected result indicates that our random control had a small unintended effect; nevertheless, significant changes in *Plp1* splicing greater than this were achieved in Oli-neu cells after treatment with sequence-specific AONs.

Morpholino Oligomer Treatment Increased Endogenous Plp1 in Oli-neu Cells

Morpholino oligomers differ from AONs in that they have a morpholine ring replacing the ribose sugar moiety and non-ionic phosphorodiamidate linkages instead of anionic phosphates, and they have been shown to be more stable, less toxic, and more efficient in similar splice-altering experiments.[54] Since our AON5 targeting the G1 and M2 regulatory sequences gave the greatest increase in *Plp*1 in our previous experiment, we designed MO-PLP to bind to the AON5 sequence in exon 3 with the addition of five bases extending in the 5′ direction to cover the *Dm20* splice site (shown in Figure 1B). Theoretically, this morpholino oligomer would have splice-altering abilities similar to AON5, but with the added hypothesized benefit of completely blocking the 5′ splice donor site for *Dm20* from the splicing machinery. Since the targeted sequence is identical in mouse and human, the morpholino oligomer could be used with either species. We treated cultured Oli-neu cells with MO-PLP or a commercially available random control morpholino oligomer (MO-RC) that has no known target or biological activity, and then we analyzed endogenous RNA levels of alternatively spliced products by RT-PCR. Treatment with MO-PLP at a concentration of 2 μM resulted in a 2.6-fold increase over untreated cells and those treated with control MO-RC (Figure 1D; Figure S1; Table S2). No effect from MO-RC nor overt toxicity was observed.

Morpholino Oligomer Treatment Switches PLP1/DM20 Alternative Splicing Expressed from Minigene-Splicing Constructs Harboring Patient Variants toward PLP1

We next wanted to determine if MO-PLP could switch the aberrant *PLP1/DM20* alternative splicing caused by patient variants toward *PLP1*. For these experiments, we used a *PLP1* minigene-splicing construct that we have used successfully in studies of *PLP1/DM20*

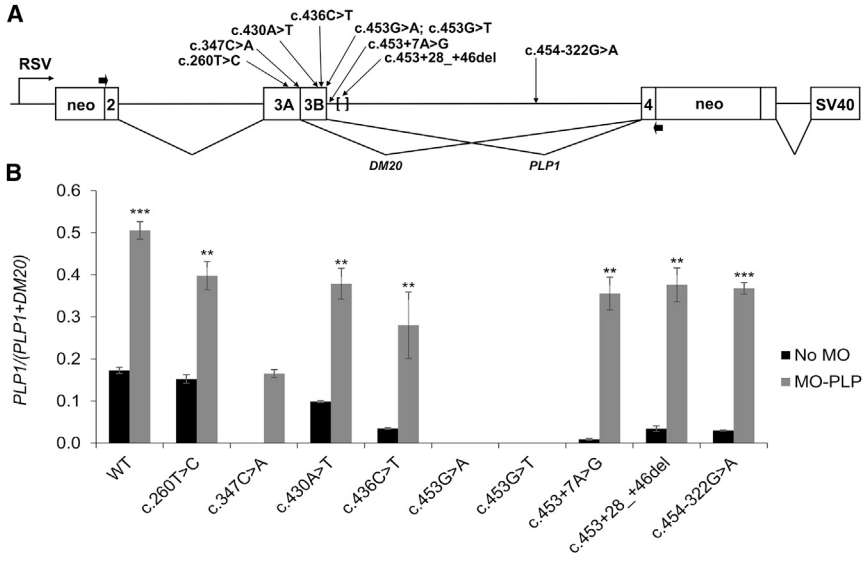

Figure 2. Modification of Alternative Splicing of *PLP1* Expressed from a Minigene-Splicing Construct Harboring PMD Patient Variants Using MO-PLP

(A) Schematic representation of the *PLP1* minigene-splicing construct, illustrating *PLP1* exon 2–4 sequence that was inserted in the neo gene and driven by the RSV promoter. The locations of the series of human variants introduced into the construct are indicated. (B) RT-PCR was performed to determine the effect of treating Oli-neu cells transfected with a series of minigene constructs harboring PMD patient variants on expression levels of the *PLP1* and *DM20* alternatively spliced products, using primers within neo-exon boundaries (represented by thick arrows in A) that amplify sequence produced by the construct and not the endogenous gene. Transfections were performed in triplicate cell cultures. Data are represented as mean ± SD; p values are for treated compared to untreated samples, *p < 0.05, **p < 0.01, and ***p < 0.001. The *PLP1* alternatively spliced product was significantly increased by treatment with MO-PLP for all constructs, except the ones where the patient variant destroys all splicing at the *PLP1* splice donor site. The capillary electrophoresis data for (B) are shown in Table S3. The primer pair used in this experiment was designed to detect *PLP1* expressed from the minigene-splicing construct and not the endogenous *Plp1* expressed in Oli-neu cells (see Figure S2).

alternative splicing (Figure 2A).[8,16] It was made by inserting a fragment of *PLP1* from part of exon 2 through part of exon 4 into the *Nco*I site in the *neo* gene of the pRSVneo plasmid. A series of constructs harboring patient variants (c.260T > C, c.347C > A, c.430A > T, c.436C > T, c.453G > A, c.453G > T, c.453+7A > G, c.453+28_+46del, and c.454-322G > A, as indicated in Figure 2A; Table 1) and a normal control construct were transfected separately into Oli-neu cells, and then the cells were either treated with MO-PLP or left untreated. The resulting levels of *PLP1* and *DM20* alternatively spliced products were determined by RT-PCR using primers that were designed to detect only plasmid-derived products (indicated by thick arrows in Figure 2A). We chose these variants for this study because they represent a spectrum of mechanisms by which *PLP1*/*DM20* alternative splicing can be disrupted.

When untreated, the *PLP1/DM20* alternative splicing was shifted away from the *PLP1* splice donor site toward the competing *DM20* site when compared to that from the normal construct (Figure 2B, black bars; Table S3), in some cases confirming our previous work, although c.260T > C compared to normal was only shifted slightly ($p > 0.05$).[8,14,16,19,30] The c.260T > C variant is in exon 3A and variants c.430A > T and c.436C > T are in exon 3B where they could create or destroy exon enhancers or silencers of *PLP1* and/or *DM20* splice site selection. The c.260T > C variant was not predicted to have an effect on alternative splicing (prediction programs SIFT,[55] PolyPhen-2,[56] Mutation Assessor,[57] Mutation Taster,[58] and FATHMM[59]), and we saw little effect on splicing (Figure 2B; Table S3). This variant changes an amino acid in *PLP1* exon 3 that is probably what causes the patient's disease, as changes in amino acids have been shown to lead to misfolded protein and ER stress.[33–35] Our data indicate that c.430A > T also caused a shift in alternative splicing away from *PLP1*, although the variant resulted in a stop codon in exon 3B. Although normal DM20 was made, no full-length PLP protein was made, probably explaining the patient's disease, as DM20 only and no PLP or DM20 (null) are known to cause disease.[36,37] The c.436C > T variant was a synonymous mutation that did not result in aberrant protein, but it did shift alternative splicing away from *PLP1*, possibly explaining the patient's disease. The c.347C > A variant strengthened the *DM20* 5′ splice donor site, shifting the *PLP1/DM20* alternative splicing away from the competing *PLP1* splice donor site toward *DM20*.[14] The c.453G > A and c.453G > T variants of the last base in exon 3 destroyed the 5′ splice donor site for the *PLP1*.[14] The c.453+7A > G variant reduced the strength of the 5′ splice donor site for the *PLP1* spliced form.[30] The 19-bp deletion variant, c.453 +28_+46del, also decreased *PLP*-specific splicing by destroying an intron splicing enhancer of *PLP*-specific splice product.[14,16] The c.454-322G > A variant, located two-thirds of the way into intron 3 of *PLP1*, decreased the *PLP*-specific form by destabilizing a long-range secondary structure that regulates alternative splicing.[8]

We showed that treatment with MO-PLP produced a significant increase in *PLP1* splicing over untreated for all the constructs that did not destroy the 5′ *PLP1* splice donor site, including the normal construct, which had an increase of 4.9-fold over untreated (Figure 2B, compare black bar to gray bar; Table S3).[14] *PLP1* expressed from the normal minigene-splicing construct in untreated Oli-neu was 17% of total *PLP1* + *DM20*, which is close to the 20% of total observed from the endogenous Oli-neu (Figure 2B compared with Figures 1C and 1D). When treated with the MO-RC, the *PLP1/DM20* alternative splicing from the normal construct and the c.453+7A > G and c.453 +28_+46del variants had no statistically significant change from when they were untreated (data not shown). From these data,

Table 1. Patient Variants Tested and/or Discussed in This Work

Patient Variant[a]	Predicted Protein[a]	Reference	Phenotype	Splicing Result
c.260T > C	p.Leu87Pro	NA	severe	not tested
c.347C > A	p.Thr116Lys	[14,19,71]	mild	strengthens *DM20* splice site
c.430A > T	p.Lys144*	[21]	classical	not tested
c.436C > T	p.(=)	[30]	mild	*PLP1/DM20* reduced to 0.18 of normal
c.436C > G	p.Leu146Val	[20,41]	mild	DM20 only detected
c.453G > A	p.(=)	[14]	severe	abolishes *PLP1*
c.453G > T	p.Lys151Asn	[14,19,20,23]	severe	abolishes *PLP1*
c.453+7A > G	p.(=)	[24,30]	classical;[24] complicated SPG2[30]	*PLP1/DM20* reduced to 0.05 of normal
c.453+28_+46del	p.(=)	[14–16]	mild	*PLP1/DM20* reduced to 0.008 of normal
c.454-322G > A	p.(=)	[8]	mild	*PLP1/DM20* reduced to 0.12 of normal

NA, not applicable.
[a]Variants were named at the RNA and protein levels using GenBank: NM_000533.3 and NP_000524.3, respectively, and using recommended nomenclature of the Human Genome Variation Society.

we conclude that MO-PLP can shift alternative splicing toward *PLP1* when splicing defects were caused by various mechanisms involved in alternative splicing, including loss of an exon splicing enhancer or intron splicing enhancer, weakening of the 5′ splice donor site for the *PLP1* spliced form, strengthening of the competing 5′ donor site for the *DM20* spliced form, and destabilization of the secondary structure in an intron. However, when a variant renders the 5′ donor site useless to produce the *PLP1* form, MO-PLP cannot overcome the defect.

Intracerebroventricular Injection of MO-PLP into a Mouse Model Normalizes Plp1/Dm20 Alternative Splicing at the RNA and Protein Levels

In the next experiment, we treated our PLP-ISEdel mouse model with MO-PLP, which we showed to be capable of shifting splicing toward *PLP1* in cell culture. The PLP-ISEdel model is a knockin of the PMD patient variant, c.453 +28_+46del, a deletion of 19 bases in intron 3 that results in reduced *Plp1* alternative splicing and a decreased amount of PLP-specific protein in the CNS, motor deficits, and microglial and astrocyte activation in the mice.[18] Our results using the minigene-splicing constructs in cell culture showed that the splicing defect caused by this variant can be ameliorated by treatment with MO-PLP (Figure 2B; Table S3), leading us to hypothesize that we could achieve similar splice-altering results *in vivo* in an animal model. Arguably, the most difficult obstacle to overcome in antisense treatment *in vivo* is the ability to dose the intended target organ or cell type without adverse effects from unintended targets or overdosing. Morpholino oligomers have been shown to be effective in many organs when administered intravenously, but they do not readily cross the blood-brain barrier. Porensky and Burghes[44] showed that a single intracerebroventricular (i.c.v.) injection in neonatal SMA mice at post-natal day 0 (P0), prior to closure of the blood-brain barrier, altered alternative splicing and that the effect lasted at least to P65. Similarly, we treated PLP-ISEdel mice by i.c.v. injection at P1–P2 with 2 μL 3 or 5 mM MO-PLP or MO-RC, and we harvested brain and spinal cord at P21, P60, and P90 for the evaluation of *Plp1/Dm20* alternative splicing. Wild-type mice and PLP-ISEdel mice that did not receive an injection were used as controls.

The single i.c.v. injection of 2 μL 3 mM MO-PLP into brains of the mice significantly increased *Plp*-specific splicing in RNA in the brains of treated PLP-ISEdel mice compared with untreated PLP-ISEdel mice at P21 (mean [SD] ratio for 3 mM MO-PLP group: 0.47 [0.11], mean [SD] ratio for untreated PLP-ISEdel group: 0.16 [0.01], t test p value = 0.04), although not reaching the level in wild-type untreated mice (Figure 3A) (mean [SD] ratio for 3 mM MO-PLP group: 0.47 [0.11], mean [SD] ratio for wild-type untreated group: 0.66 [0.01], t test p value = 0.09). The increase was sustained to P60 (mean [SD] at P60: 0.45 [0.05], P21 versus P60 t test p value = 0.83) and P90 (mean [SD] at P90: 0.33 [0.04], P21 versus P90 p value = 0.16), although the trend of the effect was down at P90. The higher dose of 5 mM MO-PLP achieved similar increases in *Plp*-specific splicing to those seen with 3 mM in brains of treated mice, so a local increase in MO-PLP concentration did not have a correlating increase in ability to alter splicing in the brain (likelihood ratio test of nested models with and without treatment p value = 0.62).

The treatment by i.c.v. injection of 3 mM MO-PLP into the brains also produced an increase in *Plp*-specific splicing in RNA from spinal cord that was comparable to what we saw in the brain at P21 (Figure 3B) (mean [SD] ratio for 3 mM P21 spinal cord group: 0.45 [0.06], 3 mM P21 brain versus spinal cord t test p value = 0.79). However, this effect decreased by P60 (mean [SD] at P60: 0.28 [0.04], P21 versus P60 spinal cord groups t test p value = 0.01) and plateaued between P60 and P90 (mean [SD] at P90: 0.26 [0.01], P60 versus P90 spinal cord groups t test p value = 0.28), which was not what was seen in brain RNA where the increase was sustained. Similarly, after i.c.v. injection of 2 μL 5 mM MO-PLP at P21 (mean [SD] = 0.52 [0.08], P21 3 versus 5 mM t test p value = 0.81), there was a significant increase in *Plp1*-specific splicing, but the increase was sustained at P60 (mean

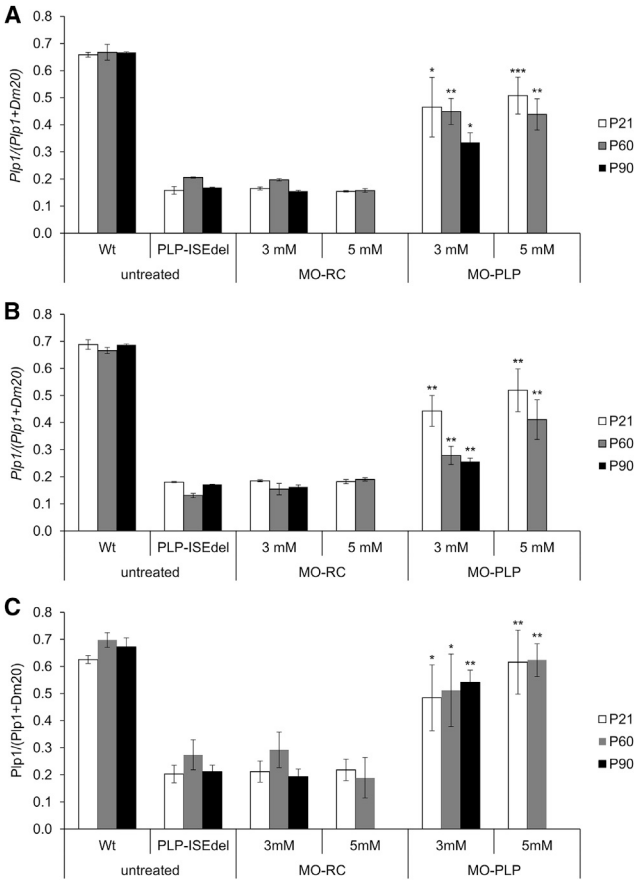

Figure 3. A Single i.c.v. Injection of MO-PLP in PLP-ISEdel Neonates Increased *Plp1* Alternatively Spliced Product in the CNS at the RNA and Protein Levels

(A and B) RT-PCR analysis of *Plp1* and *Dm20* levels was performed on RNA isolated from sagittal half brains (A) or whole spinal cord (B) of PLP-ISEdel mice harvested at P21, P60, or P90 after neonatal i.c.v. injection of 2 μL 3 mM MO-PLP or harvested at P21 or P60 after neonatal i.c.v. injection of 2 μL 5 mM MO-PLP. Protein analysis of PLP and DM20 levels was performed by western blot analysis on extracts prepared from sagittal half brains (C) after injections as above. Untreated wild-type and PLP-ISEdel controls were run on separate blots for 3-mM treatment samples and 5-mM treatment samples at each time point (see blots for 3- and 5-mM samples at P60 in Figure S4), and calculations were performed using the data from the untreated controls on the separate blots. However, only the wild-type and PLP-ISEdel samples from the P21 data for 3-mM samples are shown as representative samples on the graph. Data are represented as mean ± SD; p values are for treated compared to untreated PLP-ISEdel, *p < 0.05, **p < 0.01, and ***p < 0.001. MO-PLP-treated animals had a significantly increased *Plp1* alternatively spliced product at RNA and protein levels compared to animals treated with MO-RC. The increase in *Plp1* was sustained over time in brain. See Figures S3 and S4 for representative data.

[SD] = 0.41 [0.07], 5 mM P21 versus P60 t test p value = 0.09), as was also seen in brain RNA with 5 mM MO-PLP treatments. Even though having a local increase of MO-PLP concentration in the brain did not correlatively affect treatment response in the brain, using the higher MO-PLP concentration led to a prolonged response in the spinal cord. Treatment with the random control MO-RC did not significantly alter the amount of *Plp*-specific product in brain or spinal cord compared to PLP-ISEdel untreated controls when used at either a concentration of 3 or 5 mM (likelihood ratio test of nested models with and without treatment p value = 0.83). These results show that one i.c.v. injection of MO-PLP into neonatal brain produces a sustained increase in the *Plp*-specific splicing at the RNA level in brain and spinal cord of PLP-ISEdel mice.

Total protein preparations from treated mice and controls were used to determine if increases in *Plp*-specific RNA translated into increases in PLP-specific protein. The treatment with 2 μL of 3 or 5 mM MO-PLP by i.c.v. injection led to a significant increase in PLP protein in the brains of PLP-ISEdel animals compared to the untreated PLP-ISEdel controls at P21 (mean [SD] of 3 mM group = 0.48 [0.12], mean [SD] of untreated PLP-ISEdel = 0.27 [0.06], 3 mM versus untreated PLP-ISEdel t test p value = 0.02; mean [SD] of 5 mM group = 0.62 [0.12], mean [SD] of untreated PLP-ISEdel = 0.20 [0.03], 5 mM versus untreated PLP-ISEdel t test p value = 0.01), which was sustained to P60 (mean [SD] of P60 3 mM group = 0.52 [0.13], P21 versus P60 3 mM group t test p value = 0.78; mean [SD] of P60 5 mM group = 0.62 [0.06], P21 versus P60 5 mM group t test p value = 0.91) and to P90 at 3 mM (mean [SD] of P90 3 mM group = 0.54 [0.04], P21 versus P90 3 mM group t test p value = 0.44) (5 mM was not tested at P90) (Figure 3C). Examination of the animals treated with 5 mM MO-PLP revealed similar results to those with the 3-mM treatments. Treatment of PLP-ISEdel with 2 μL 3 or 5 mM random control MO-RC did not significantly change PLP-specific protein levels compared to untreated PLP-ISEdel in brain samples at any time point examined (likelihood ratio test of nested models with and without treatment p value = 0.97). These results show that one i.c.v. injection of MO-PLP into neonatal brain produced a sustained increase in PLP at the protein level in brains of PLP-ISEdel mice.

There Was a Sustained Decrease in Inflammatory Markers after Treatment of PLP-ISEdel Mice with MO-PLP

The PLP-ISEdel mouse line was shown to have an increase in histological markers of astrocytes and microglia in white matter of the brain as early as 2 months, which increases and progresses to gray matter by 4 months.[60] These changes were accompanied by motor impairment on the rotarod and in the open field. Since inflammation is damaging to axons, maybe even more damaging than hypomyelination, and axonal damage correlates with severity of disease symptoms,[61,62] we asked whether inflammation in the brains of PLP-ISEdel mice could be ameliorated by i.c.v. injection of MO-PLP. First, we investigated the mRNA levels of four markers of inflammation that were found among the most highly increased in a model of Alzheimer[63] and our *Plp1*dup model of the PMD duplication[64] (data not shown): *Cst7* (cystatin F); the chemokine *Ccl3*; *Itgax*; and *Gfap*, an astrocyte marker that is increased in reactive astrocytes. Expression from all four genes was elevated in brains of PLP-ISEdel mice with respect to wild-type at both P60 (one-sample t test with null hypothesis of mu = 1: p value for *Ccl3* = 0.003, p value for *Cst7* = 0.007, p value for *Gfap* = 0.02, and p value for *Itgax* = 0.008) and P90

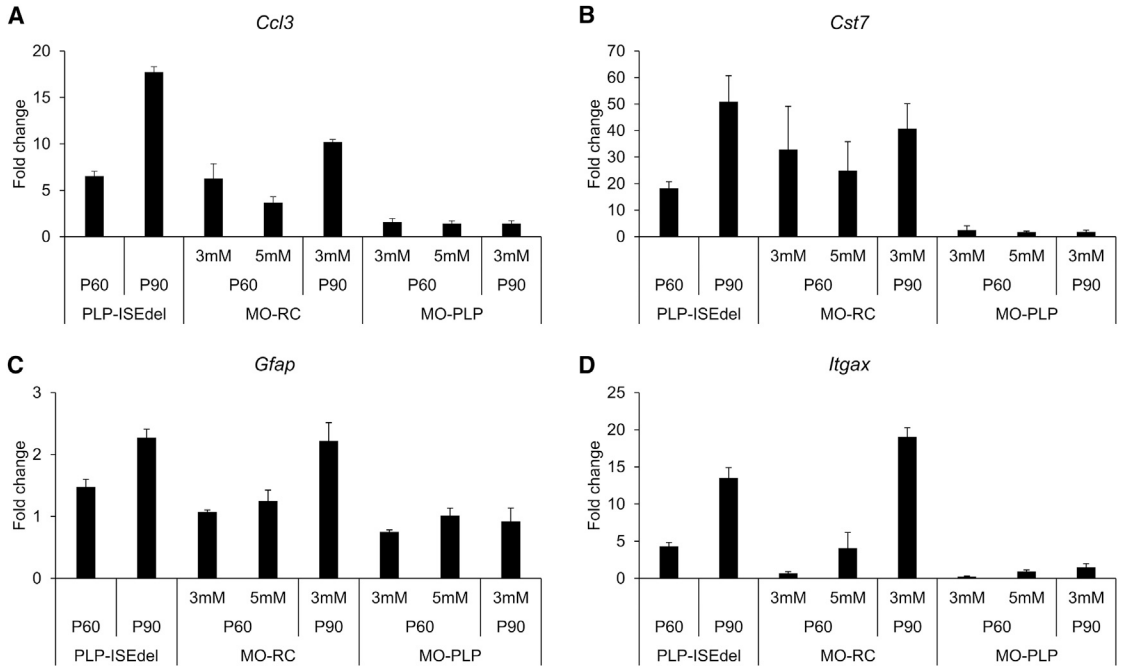

Figure 4. A Single i.c.v. Injection of MO-PLP in PLP-ISEdel Neonates Decreased Expression of Inflammatory Markers

(A–D) qRT-PCR analysis of expression levels of four inflammatory markers, (A) *Ccl3*, (B) *Cst7*, (C) *Itgax*, and (D) *Gfap*, in RNA from sagittal half brains harvested at P21, P60, or P90 after neonatal i.c.v. injection of 2 μL 3 mM MO-PLP or harvested at P21 or P60 after neonatal i.c.v. injection of 2 μL 5 mM MO-PLP (the same RNA that was used for the experiment in Figure 3). Data are expressed as fold change relative to wild-type. Experiments were performed with triplicate reactions on 3–5 biological replicates of each condition (age, genotype, and treatment). MO-PLP treatment produced a sustained reduction of inflammatory markers.

(one-sample t test with null hypothesis of mu = 1: p value for *Ccl3* = 0.0004, p value for *Cst7* = 0.01, p value for *Gfap* = 0.004, and p value for *Itgax* = 0.004), but not at P21 (Figure 4; P21 data not shown). PLP-ISEdel mice injected with 3 or 5 mM MO-PLP at P1/P2 had significantly lower levels of the four inflammatory markers at P60 (one-sample t test with null hypothesis of mu = 1: p value for *Ccl3* = 0.003, p value for *Cst7* = 0.007, p value for *Gfap* = 0.02, and p value for *Itgax* = 0.008). Levels of *Cst7* and *Ccl3* remained low at P90 (P60 versus P90 likelihood ratio test for *Ccl3* = 0.48; P60 versus P90 likelihood ratio test for *Cst7* = 0.27). Mice treated with the 3 mM random control MO-RC at P1/P2 showed some decrease of *Gfap* and *Itgax* at P60 (difference in *Ccl3* between PLP-ISEdel and MO-RC at P60 from t test p value = 0.81; difference in *Cst7* between PLP-ISEdel and MO-RC at P60 from t test p value = 0.26; difference in *Gfap* between PLP-ISEdel and MO-RC at P60 from t test p value = 0.02; and difference in *Itgax* between PLP-ISEdel and MO-RC at P60 from t test p value = 0.002), and decreases of *Cst7* and *Itgax* at P90 (difference in *Ccl3* between PLP-ISEdel and MO-RC at P90 from t test p value = 0.0004; difference in *Cst7* between PLP-ISEdel and MO-RC at P90 from t test p value = 0.26; difference in *Gfap* between PLP-ISEdel and MO-RC at P90 from t test p value = 0.81; and difference in *Itgax* between PLP-ISEdel and MO-RC at P90 from t test p value = 0.007; MO-RC higher than PLP-ISEdel), suggesting that either the random control or the injection itself may have had some effect on inflammation, but the effect was small. Thus, a single i.c.v. injection of MO-PLP at P1/P2 ameliorated the inflammatory response in PLP-ISEdel mice and the effect was sustained to P90. Sustained increases in *Plp*-specific splicing at both the RNA and protein levels (Figure 3) and sustained amelioration of the inflammatory response with i.c.v. injections (Figure 4) suggest that MO-PLP is a good candidate drug for correcting aberrant alternative splicing of *PLP1* causing PMD, SPG2, and HEMS in patients.

DISCUSSION

Antisense oligomer splice alteration is increasingly becoming an exciting approach for the treatment of diseases that occur because of splicing defects. Antisense drugs for several diseases, SMA and Duchenne muscular dystrophy (DMD) in particular, are currently being used in clinical trials to test efficacy *in vivo* (reviewed in Havens and Hastings[42]). FDA approval has been granted recently for one of these drugs, nusinersen (Spinraza) for the treatment of SMA, following a successful phase 2 clinical trial.[48] In our investigation, we sought to determine whether antisense oligomers could be used as a treatment to overcome alternative splicing defects that are a cause of the neurodegenerative diseases PMD, SPG2, and HEMS. We first tested a series of antisense RNA oligomers in cultured Oli-neu cells to determine target sequences for altering the alternative splicing of *Plp1/Dm20* expressed from the endogenous *Plp1* gene. We found that the *Dm20* splice site was a good target for shifting alternative splicing toward *Plp1*, and we showed that a morpholino oligomer, MO-PLP, designed to bind at the *Dm20* splice donor site, dramatically increased *Plp*-specific splicing in Oli-neu cell culture. Treatment

with MO-PLP also increased *PLP*-specific splicing when minigene constructs with alternative splicing defects caused by various *PLP1* gene variants were transfected into cultured Oli-neu cells. Furthermore, treatment by i.c.v. injection of MO-PLP into brains of the mouse model PLP-ISEdel, which has a 19-bp deletion of a splicing enhancer for *PLP*-specific splicing, normalized the *PLP1*/*DM20* alternative splicing defect. We also demonstrated that correction of splicing in the mouse model was long-lasting, and it resulted in the improvement of a previously reported inflammatory phenotype.[60]

Our work and that of others suggest that exons 3A and 3B and intron 3 of *PLP1* are rich with sequences that affect *PLP1*/*DM20* alternative splicing by enhancing or silencing splicing at the *DM20* and/or *PLP1* splice donor sites or by interacting with general splicing factors of the transcriptional machinery (Figure 1).[8,14–18,30,41,52,53] For example, an exon splicing enhancer containing a putative ASF/SF2 motif that leads to preferential *PLP1* 5′ splice site selection was identified in exon 3B of *PLP1*, and variants in this element result in reduced *PLP1* 5′ splice site selection.[17] Conversely, a region in exon 3B was identified as an enhancer of *DM20* 5′ splice site selection, and, when mutated, it leads to an increase in *PLP1* mRNA splice product.[52] A 19-bp G-rich element acting as an intron splicing enhancer that influences splicing in favor of *PLP1* was found in *PLP1* intron 3.[16,53] We showed that patient variants within exon 3 or intron 3 that reduce the *PLP1* alternatively spliced product, even those that do not result in amino acid changes, can cause PMD or HEMS.[8,16,30] Thus, it is likely that variants in these regions can affect alternative splicing either by destroying regulatory elements for splicing or by creating additional regulatory elements.

With so many splice regulatory elements in the region of the *PLP1*/*DM20* alternative splice in PMD patients, it is theoretically possible to tailor treatments with morpholino oligomers to alter the specific deficiency in splicing depending on the patient's own variant. Indeed, an antisense approach for correction of alternative splicing caused by the c.436C > G variant of *PLP1* was previously reported by Regis et al.[41] This variant is in the exon 3B portion of *PLP1* that is spliced out in formation of the *DM20* alternative form (see Figure 2A). The authors determined that the variant affected splicing by creating exon splicing silencer (ESS) motifs that eliminated splicing from the *PLP1* splice donor site. They corrected the splicing defect by targeting the motifs with an antisense morpholino oligomer that blocked the motifs, thereby increasing splicing from the *PLP1* splice donor site.

Advantages of our approach over that of Regis et al.[41] are that it works for a variety of *PLP1* variants and no knowledge of the mode of action for any particular variant on splicing is necessary. Approximately 12% of published PMD point mutations and insertions or deletions (indels) are in exon or intron 3, where they have the potential to reduce without abolishing *PLP*-specific splicing,[65] although the effect on alternative splicing has not been tested for many of them. It should be noted, however, that many diagnostic labs do not sequence intron 3 of *PLP1*, so the estimate is probably low. In this paper, we have demonstrated switching of alternative splicing toward *PLP1* for seven *PLP1* variants using our MO-PLP antisense morpholino oligomer, which was designed to block the *DM20* splice donor site. The only variants tested for which MO-PLP did not affect alternative splicing were those that actually destroyed the *PLP1* splice donor site sequence itself. Although we did not test our approach on the c.436C > G variant corrected by Regis et al.,[41] our MO-PLP would be expected to switch splicing toward *PLP1* for this variant, as we did test c.436C > T, a different change of the same base as in Regis et al.,[41] and splicing was switched toward *PLP1*. It is worth noting that our MO-PLP could be used in combination with antisense oligomers targeting existing or created splice enhancer or silencer sequences like the one used by Regis et al.[41] for more careful modulation of *PLP1*/*DM20* alternative splicing.

Our MO-PLP is most likely to be therapeutic for patients who have synonymous exonic variants or variants in intron 3 that reduce *PLP1* splicing, because these variants would produce completely normal *PLP1* and *DM20* products when splicing is corrected. Notably, one of the synonymous exonic patient variants that we tested and found to be corrected by MO-PLP is c.436C > T that is a different change of the same base as the variant corrected in Regis et al.,[41] which is not a synonymous variant. Variants within intron 3 that can be treated with MO-PLP are of three types: those that weaken but do not eliminate the *PLP1* splice donor sequence; those that disrupt an intron splicing enhancer like the c.453+28_+46del variant in our PLP-ISEdel mouse model, which we used for preclinical testing in this report;[18] and those that affect previously described long-distance interacting sequences (LDISs) deep within intron 3, which keep them from forming a secondary structure like c.454-322G > A.[8]

Our MO-PLP may also prove to be therapeutic for some patients whose variants reduce PLP product but are exonic variants that would be expected to result in a mutant PLP protein when splicing is corrected. Regis et al.[41] provide a reasonable rationale for the therapeutic potential of increasing *PLP1* in patients with the c.436C > T variant that results in a mutant PLP protein. Briefly, patient variants in exon 3B that change amino acids without additionally affecting alternative splicing typically result in relatively mild disease when compared with those in other *PLP1* exons. If the variant is mild enough, having more of that mild mutant PLP protein may result in a milder phenotype than having no PLP or only a small amount of PLP.

Our MO-PLP may prove to be therapeutic for the c.347C > A variant that strengthens the *DM20* splice site, but again, the variant results in a mutant PLP protein, so the discussion in the previous paragraph applies. It may also prove to be therapeutic for the patient with the c.430A > T variant and others whose variants result in truncated PLP protein, if having little PLP due to a splicing error causes a more severe phenotype than having more of a truncated PLP. Further testing would need to be done to determine if there are any patients whose variants result in truncated PLP, but not a splicing defect, for comparison with those whose variants result in both.

The *in vivo* effect of complete redirection of splicing from 70% PLP and 30% DM20 to 100% PLP1 is not known. Although there is a phenotype described for DM20 only mice,[13,66] there have been no mammals generated in which PLP is the only isoform expressed. Amphibians normally make only the PLP form despite having a high degree of sequence similarity with mammals in the region of the alternative splice,[67] so it could be argued that PLP only should not be detrimental in mammals. However, this is not a totally satisfactory argument because amphibians also express P0 in their CNS, which is the major protein in the peripheral nervous system (PNS) of mammals, so P0 may compensate for the lack of DM20. Thus, it remains possible that too great a shift or a complete shift from the normal 70% to 100% could be detrimental if the DM20 isoform is needed for normal function, if extra PLP isoform is toxic, or both. It is of note, however, that the MO-PLP morpholino oligomer did not completely redirect splicing from *DM20* to *PLP1* in our cell culture or mouse experiments.

There are several considerations for the application of antisense treatments for HEMS in a clinical setting. The onset of symptoms is typically in late infancy,[30] so treatment would need to be given early to prevent disease. Once damage to the CNS has occurred, it is not likely to be repaired; however, later treatment may halt progression. Intrathecal delivery of antisense oligomers that alter splicing has proven to be efficacious and safe in SMA patients, so risks for treatment of HEMS by the same route seem minimal. It is likely that successive treatments would need to be given for maintenance. Strategies for a treatment regimen for SMA patients are now being tested, and these studies should inform treatment regimen strategies for PMD, SPG2, and HEMS patients.

Of the several antisense oligonucleotide drugs that have received FDA approval and reached the market, none has yet been commercially successful. In any case, the studies leading to the development of these drugs and others have led to technological advances in oligonucleotide design and delivery methods. Recently, the encouraging results in clinical trials and FDA approval of splice-modifying drugs for the treatment of SMA and DMD suggest that a commercially successful antisense oligonucleotide drug may be on the horizon.[48,68] Perhaps success with antisense technology on diseases with relatively large numbers of patients will then drive testing of antisense oligonucleotide drugs for private patient variants or small classes of variants. Our studies demonstrate the feasibility of an antisense oligonucleotide approach as a treatment for the ultra-rare class of *PLP1* variants that causes disease by altering alternative splicing.

MATERIALS AND METHODS

Animals

The PLP-ISEdel mouse model was generated using the hit-and-run strategy as described, so that the 19-bp deletion of *Plp1* intron 3 bases +28 to +46 is the only variant introduced during generation of the model.[18] Animal work was approved by the Nemours Institutional Animal Care and Use Committee (IACUC) and with its oversight. The work was also in accordance with the U.S. Public Health Service Policy on Humane Care and Use of Laboratory Animals (Office of Laboratory Animal Welfare, 2013) and the *Guide for the Care and Use of Laboratory Animals* (Office of Laboratory Animal Welfare, 2013). ARRIVE guidelines and NIH recommendations calling for transparent reporting were used in the preparation of the manuscript. All mice used were males on a C57BL/6 background. Mice were provided water and standard mouse chow *ad libitum*.

Minigene-Splicing Constructs, Antisense Oligomers, and Morpholino Oligomers

The minigene-splicing construct was generated, plasmid DNA was produced, and single-base patient variants were introduced as described.[8] AONs were synthesized by Integrated DNA Technologies (IDT, Coralville, IA, USA), and morpholino oligomers were synthesized by Gene Tools (Pilomath, OR, USA). The RNA antisense sequences covered by AONs across and near the *DM20* splice site and the morpholino oligo antisense sequence of MO-PLP can be deduced from the sequences indicated by underline in Figure 1B. The sequence of the random control AON, AON-RC, was 5′-CGUG CACCCUCUCGCGCUUG-3′. MO-RC was the commercially available random control 25-N morpholino, which is a mixture of oligomer sequences produced by the addition of a mixture of morpholino subunits at each step of the synthesis cycle (Gene Tools).

Cell Culture and Transfections

Cell culture was performed as described.[8] Transfection of plasmid DNA was performed as follows: Oli-neu cells (1.2×10^5)[49] were plated in each well of a poly-L-Lysine-coated 12-well plate on day 1. Plasmid DNAs (1.2 μg DNA/well) prepared using EndoFree Plasmid Maxi Kit (QIAGEN, Valencia, CA, USA) were transfected on day 2 using Lipofectamine 2000 (Invitrogen), according to the manufacturer's protocol. After 4–5 hr, incubation medium was removed and replaced with fresh medium containing 2 μM MO-PLP and 2 μM EndoPorter (Gene Tools), according to the manufacturer's protocol. On day 3, 24 hr after the addition of morpholino, the medium was removed, in-well lysis and homogenization were performed using a QIAshredder Kit (QIAGEN, Valencia, CA, USA) according to the manufacturer's protocol, and samples were stored at −80°C or immediately processed for RNA isolation. Transfection of antisense oligomers was performed as follows: cells (1.1×10^5) were plated in each well of a 6-well poly-L-Lysine-coated plate on day 1. Antisense oligomers (40 nM) were transfected on day 2 using Lipofectamine 2000, according to the manufacturer's protocol. After 4–5 hr the medium was replaced with fresh medium, and after 24 hr the medium was removed, in-well lysis and homogenization were performed, and samples were stored and processed as mentioned above. All transfections were performed in triplicate.

Treatment of Mouse Model with Morpholino Oligomers by i.c.v. Injection

At least four animals were used for each treatment group and morpholino concentration for *in vivo* experiments. PLP-ISEdel mice were given markings with tattoo in footpads at P0–P1 (P0 defined as day of birth), and tail snips were taken for PCR-based genotyping

and sex determination as described.[64] Care was taken to discourage maternal abandonment by rubbing hands thoroughly in soiled bedding to obtain home cage scent on the handler's gloves. Animals were randomly assigned to treatment groups, and all male animals in a litter that were entered into the experiment were given the same treatment. The i.c.v. injection of mice was performed as described[69] at P1 or P2 with 2 μL of either 3 or 5 mM of either MO-PLP (Figure 1B) or MO-RC (random control 25-N provided by Gene Tools).

Briefly, morpholino oligomers were mixed with 0.05% w/v trypan blue in PBS for visualization of the injection site and spread throughout the CNS. Cryo-anesthesia was used to immobilize mice for 1–2 min for injections. Mice were placed on a light source for clear visualization of brain structures while a needle was inserted to a depth of 2 mm 0.25 mm lateral of the sagittal suture and 0.50–0.75 mm rostral of the neonatal coronary suture. Backflow into the needle was prevented by holding it in place for 15 s. Mice were placed in a warmed container for 5–10 min for recovery after the injection, and they were monitored until they returned to normal movement and responsiveness. Approximately the same numbers of injected male pups and untreated female pups died prior to weaning. Animals were euthanized by CO_2 inhalation at P21 (median, P21; range, P21–P22), P60 (median, P60; range, P60–P61), or P90 (median, P90; range, P89–P90, one P104). Brains and spinal cords were isolated and batched for RNA and protein analysis, and tail snips were used to confirm genotyping.

RNA Extraction and Semiquantitative RT-PCR

RNA was isolated from Oli-neu cells as described[8] and from mouse brain as described.[64] *Plp1* and *Dm20* alternatively spliced transcript levels produced from the endogenous mouse *Plp1* gene in Oli-neu cells and in mouse brain were measured by semiquantitative RT-PCR. Reverse transcription was performed using the Omniscript reverse transcription kit (QIAGEN), following the manufacturer's protocols. PCR amplification was performed with the Multiplex PCR Kit (QIAGEN), according to the manufacturer's protocol. Products were detected and analyzed by capillary electrophoresis using the 3130 xL Genetic Analyzer (Invitrogen) and Peak Scanner Software or the 3500 Genetic Analyzer system (Invitrogen) with Genemapper software (Applied Biosystems). The primer pair used to detect both endogenous *Plp1* and *Dm20* in the same reaction was mPLP2F (5′-GTTGTGCTAGATGTCTGGTAGG-3′) and 6-FAM-labeled mPLP4R (5′-AGCCATACAACAGTCAGGGCATAG-3′) (Figure S2). The primer pair used to detect *PLP1* and *DM20* produced from the constructs and not the endogenous signal was neo-ex2F (5′-GTCGTGACCCATGGCACAGAAA-3′ [M83237.1, 3,814–3,828; Z73964.2, 15,262–15,271]) and 6-FAM-labeled neo-ex4R (5′-CATC GCCATGGGTGATGCC-3′ [M83237.1, 3,832–3,820; Z73964.2, 17,366–17,372]) (Figure S2). These primers spanned the junction from the neo gene in the construct into the *PLP1* insert. A primer pair in the Cyclophilin A gene, 5′-ACCCCACCGTGTTCTTC GAC-3′ and 6-FAM-labeled 5′-CATTTGCCATGGACAAGATG-3′, was used as an amplification and loading control in all RT-PCR reactions.

Protein Extraction and Western Blot Analysis

Proteins were extracted from sagittal half-brain homogenates using a buffer containing 150 mM NaCl, 50 mM Tris-HCl, 1% Triton X-100, 5 mM EDTA, 0.1% SDS, and 1% sodium deoxycolate freshly supplemented with Halt Protease Inhibitor Cocktail (Thermo Scientific, Rockford, IL, USA), and they were measured by BCA Protein Assay (Thermo Scientific). Proteins were separated by gradient SDS-PAGE (4%–20% TGX, Bio-Rad) and blotted onto polyvinylidene fluoride (PVDF) membrane (Invitrogen). Western blots were probed with antibodies to PLP/DM20 (1:2,000, AA3 Hybridoma) and GAPDH (1:50,000, Sigma-Aldrich), followed by horseradish peroxidase (HRP)-conjugated secondary antibody (1:5,000, Jackson ImmunoResearch), and detected using SuperSignal West Femto ECL (Thermo Scientific). Bands were visualized using C-DiGit Chemiluminescent Blot Scanner (LI-COR Biosciences, Lincoln, NE, USA) and quantified using iS Image Studio Version 4.0 (LI-COR Biosciences).

RNA Isolation and qRT-PCR

RNA from mouse brains was isolated and treated with DNase as described.[64] RNA concentration was measured with the NanoDrop (Thermo Fisher Scientific), and the integrity of the RNA was measured on the Agilent 2100 Bioanalyzer. Only RNAs with RNA integrity number (RIN) > 7.6 were used in further analysis. cDNA was obtained using Applied Biosystems High-Capacity reverse transcription kit including Promega's RNasin RNase inhibitor. PrimeTime predesigned probe-based qPCR assays (IDT) were used with QuantiTect Probe PCR Master mix (QIAGEN), following the manufacturer's instructions, to assess transcript levels on inflammatory markers chemokine (C-C motif) ligand 3 (*Ccl3*, Mm.PT.58.29283216), cystatin F (*Cst7*, Mm.PT.58.8810317), glial fibrillary acidic protein (*Gfap*, Mm.PT.58.6609337), and integrin alpha X (*Itgax*, Mm.PT.58.42516719). Assays on calnexin (*Canx*, Mm.PT.58.6272785) and cytochrome *c*-1 (*Cyc1*, Mm.PT.56a.33431602.gs) were included as reference genes based on previous experiments.[64] Experiments were performed with triplicate reactions on three to four biological replicates of each condition (age, genotype, and treatment). Reactions were analyzed using the ABI 7900HT Fast Real-Time PCR System (Invitrogen) with SDS 2.3 software (Invitrogen), following the procedure previously described.[64] The Ct values for each sample were divided by the mean of the Ct values of the internal reference genes Canx and Cyc1 for normalization. Relative quantification (RQ) of transcript levels of the inflammatory marker genes was determined using the wild-type males as the calibrator with SDS 2.3 software (Invitrogen) with the $2^{\Delta\Delta Ct}$ method.

Statistical Analyses

The RT-PCR data for the Oli-neu cell culture studies in Figures 1C and 1D (see also Tables S1 and S2) and Figure 2B (see also Table S3) were summarized using means and SDs. Comparisons of treated and untreated samples were carried out using two-sample unpaired t test assuming unequal variance. Analyses were two-tailed with the level of significance at 5%.

Protein and RNA levels for the mouse treatment studies in Figures 3 and 4 were summarized using means and SDs. Comparison of each outcome at the same time point between groups was carried out using one-way ANOVA or two-sample unpaired t test assuming unequal variance. One-sample t test was used to detect fold changes in each of the inflammatory marker genes using RQ with the expression in wild-type as 1. Analysis on changes in an outcome across time points for the same group was carried out in the same way. Comparison of an outcome across time points between groups was carried out using multi-way ANOVA, accounting for site (brain and spinal cord), treatments, and time point. To test the presence of treatment effect, nested models with and without the treatment variable were compared using likelihood ratio test. All analyses were two tailed with the level of significance at 5%. All statistical analysis was performed using R Statistical Software, version 3.3.1.[70]

SUPPLEMENTAL INFORMATION

Supplemental Information includes four figures and three tables and can be found with this article online at https://doi.org/10.1016/j.omtn.2018.05.019.

AUTHOR CONTRIBUTIONS

Conceptualization, G.M.H., S.T., and K.S.; Methodology, G.M.H., S.T., K.S., and J.T.; Validation, S.T., K.S., and J.T.; Formal Analysis, G.M.H., S.T., J.T., and K.S.; Investigation, G.M.H., S.T., K.S., J.T., and K.K.; Writing – Original Draft, S.T. and G.M.H.; Writing – Review & Editing, G.M.H., S.T., K.S., J.T., and K.K.; Visualization, S.T. and G.M.H.; Supervision, G.M.H.; Funding Acquisition, G.M.H.

ACKNOWLEDGMENTS

We acknowledge the Nemours Biomolecular Core (supported by NIH grants P30GM114736 and P20GM103446), the Nemours Bioinformatics Core (Sherlly Xie, Biostatistician), and the Nemours Molecular Diagnostics Laboratory for contributions to this work. We thank Anne Hesek for assistance with the animal work. This work was supported by the NIH (P30GM114736 and R01NS058978 to G.M.H.) and the PMD Foundation (to G.M.H.). The content is solely the responsibility of the authors and does not necessarily represent the official views of the granting agencies and foundations.

The authors acknowledge first author, colleague, and friend Stephanie Tantzer, who died after the work for this article was completed.

REFERENCES

1. Cartegni, L., Chew, S.L., and Krainer, A.R. (2002). Listening to silence and understanding nonsense: exonic mutations that affect splicing. Nat. Rev. Genet. *3*, 285–298.
2. Ward, A.J., and Cooper, T.A. (2010). The pathobiology of splicing. J. Pathol. *220*, 152–163.
3. Johnson, J.M., Castle, J., Garrett-Engele, P., Kan, Z., Loerch, P.M., Armour, C.D., Santos, R., Schadt, E.E., Stoughton, R., and Shoemaker, D.D. (2003). Genome-wide survey of human alternative pre-mRNA splicing with exon junction microarrays. Science *302*, 2141–2144.
4. Orengo, J.P., and Cooper, T.A. (2007). Alternative splicing in disease. Adv. Exp. Med. Biol. *623*, 212–223.
5. Matlin, A.J., Clark, F., and Smith, C.W. (2005). Understanding alternative splicing: towards a cellular code. Nat. Rev. Mol. Cell Biol. *6*, 386–398.
6. Buratti, E., and Baralle, F.E. (2004). Influence of RNA secondary structure on the pre-mRNA splicing process. Mol. Cell. Biol. *24*, 10505–10514.
7. Shepard, P.J., and Hertel, K.J. (2008). Conserved RNA secondary structures promote alternative splicing. RNA *14*, 1463–1469.
8. Taube, J.R., Sperle, K., Banser, L., Seeman, P., Cavan, B.C., Garbern, J.Y., and Hobson, G.M. (2014). PMD patient mutations reveal a long-distance intronic interaction that regulates PLP1/DM20 alternative splicing. Hum. Mol. Genet. *23*, 5464–5478.
9. Zhang, J., Kuo, C.C., and Chen, L. (2011). GC content around splice sites affects splicing through pre-mRNA secondary structures. BMC Genomics *12*, 90.
10. Nave, K.A., Lai, C., Bloom, F.E., and Milner, R.J. (1987). Splice site selection in the proteolipid protein (PLP) gene transcript and primary structure of the DM-20 protein of central nervous system myelin. Proc. Natl. Acad. Sci. USA *84*, 5665–5669.
11. LeVine, S.M., Wong, D., and Macklin, W.B. (1990). Developmental expression of proteolipid protein and DM20 mRNAs and proteins in the rat brain. Dev. Neurosci. *12*, 235–250.
12. Timsit, S.G., Bally-Cuif, L., Colman, D.R., and Zalc, B. (1992). DM-20 mRNA is expressed during the embryonic development of the nervous system of the mouse. J. Neurochem. *58*, 1172–1175.
13. Stecca, B., Southwood, C.M., Gragerov, A., Kelley, K.A., Friedrich, V.L., Jr., and Gow, A. (2000). The evolution of lipophilin genes from invertebrates to tetrapods: DM-20 cannot replace proteolipid protein in CNS myelin. J. Neurosci. *20*, 4002–4010.
14. Hobson, G.M., Huang, Z., Sperle, K., Sistermans, E., Rogan, P.K., Garbern, J.Y., Kolodny, E., Naidu, S., and Cambi, F. (2006). Splice-site contribution in alternative splicing of PLP1 and DM20: molecular studies in oligodendrocytes. Hum. Mutat. *27*, 69–77.
15. Hobson, G.M., Davis, A.P., Stowell, N.C., Kolodny, E.H., Sistermans, E.A., de Coo, I.F.M., Funanage, V.L., and Marks, H.G. (2000). Mutations in noncoding regions of the proteolipid protein gene in Pelizaeus-Merzbacher disease. Neurology *55*, 1089–1096.
16. Hobson, G.M., Huang, Z., Sperle, K., Stabley, D.L., Marks, H.G., and Cambi, F. (2002). A PLP splicing abnormality is associated with an unusual presentation of PMD. Ann. Neurol. *52*, 477–488.
17. Wang, E., Huang, Z., Hobson, G.M., Dimova, N., Sperle, K., McCullough, A., and Cambi, F. (2006). PLP1 alternative splicing in differentiating oligodendrocytes: characterization of an exonic splicing enhancer. J. Cell. Biochem. *97*, 999–1016.
18. Wang, E., Dimova, N., Sperle, K., Huang, Z., Lock, L., McCulloch, M.C., Edgar, J.M., Hobson, G.M., and Cambi, F. (2008). Deletion of a splicing enhancer disrupts PLP1/DM20 ratio and myelin stability. Exp. Neurol. *214*, 322–330.
19. Shy, M.E., Hobson, G., Jain, M., Boespflug-Tanguy, O., Garbern, J., Sperle, K., Li, W., Gow, A., Rodriguez, D., Bertini, E., et al. (2003). Schwann cell expression of PLP1 but not DM20 is necessary to prevent neuropathy. Ann. Neurol. *53*, 354–365.
20. Grossi, S., Regis, S., Biancheri, R., Mort, M., Lualdi, S., Bertini, E., Uziel, G., Boespflug-Tanguy, O., Simonati, A., Corsolini, F., et al. (2011). Molecular genetic analysis of the PLP1 gene in 38 families with PLP1-related disorders: identification and functional characterization of 11 novel PLP1 mutations. Orphanet J. Rare Dis. *6*, 40.
21. Bartholomew, D.W., and McClellan, J.M. (1998). A novel mutation in the variably spliced region of the human PLP gene associated with classical Pelizaeus-Merzbacher disease, Mutation and Polymorphism Report #17. Hum. Mutat. *12*, 220.
22. Laukka, J.J., Stanley, J.A., Garbern, J.Y., Trepanier, A., Hobson, G., Lafleur, T., Gow, A., and Kamholz, J. (2013). Neuroradiologic correlates of clinical disability and progression in the X-linked leukodystrophy Pelizaeus-Merzbacher disease. J. Neurol. Sci. *335*, 75–81.
23. Pratt, V.M., Naidu, S., Dlouhy, S.R., Marks, H.G., and Hodes, M.E. (1995). A novel mutation in exon 3 of the proteolipid protein gene in Pelizaeus-Merzbacher disease. Neurology *45*, 394–395.
24. Hübner, C.A., Orth, U., Senning, A., Steglich, C., Kohlschütter, A., Korinthenberg, R., and Gal, A. (2005). Seventeen novel *PLP1* mutations in patients with Pelizaeus-Merzbacher disease. Hum. Mutat. *25*, 321–322.
25. Pratt, V.M., Trofatter, J.A., Larsen, M.B., Hodes, M.E., and Dlouhy, S.R. (1992). New variant in exon 3 of the proteolipid protein (PLP) gene in a family with Pelizaeus-Merzbacher disease. Am. J. Med. Genet. *43*, 642–646.

26. Bridge, P.J., and Wilkins, P.J. (1992). The role of proteolipid protein gene mutations in Pelizaeus-Merzbacher disease. Am. J. Hum. Genet. *51*, A209.

27. Laššuthová, P., Žaliová, M., Inoue, K., Haberlová, J., Sixtová, K., Sakmaryová, I., Paděrová, K., Mazanec, R., Zámečník, J., Šišková, D., et al. (2014). Three new PLP1 splicing mutations demonstrate pathogenic and phenotypic diversity of Pelizaeus-Merzbacher disease. J. Child Neurol. *29*, 924–931.

28. Osaka, H., Koizume, S., Aoyama, H., Iwamoto, H., Kimura, S., Nagai, J., Kurosawa, K., and Yamashita, S. (2010). Mild phenotype in Pelizaeus-Merzbacher disease caused by a PLP1-specific mutation. Brain Dev. *32*, 703–707.

29. Cailloux, F., Gauthier-Barichard, F., Mimault, C., Isabelle, V., Courtois, V., Giraud, G., Dastugue, B., and Boespflug-Tanguy, O.; Clinical European Network on Brain Dysmyelinating Disease (2000). Genotype-phenotype correlation in inherited brain myelination defects due to proteolipid protein gene mutations. Eur. J. Hum. Genet. *8*, 837–845.

30. Kevelam, S.H., Taube, J.R., van Spaendonk, R.M., Bertini, E., Sperle, K., Tarnopolsky, M., Tonduti, D., Valente, E.M., Travaglini, L., Sistermans, E.A., et al. (2015). Altered PLP1 splicing causes hypomyelination of early myelinating structures. Ann. Clin. Transl. Neurol. *2*, 648–661.

31. Hobson, G.M., and Garbern, J.Y. (2012). Pelizaeus-Merzbacher disease, Pelizaeus-Merzbacher-like disease 1, and related hypomyelinating disorders. Semin. Neurol. *32*, 62–67.

32. Hobson, G.M., and Kamholz, J. (2013). *PLP1*-Related Disorders. In GeneReviews, M.P. Adam, H.H. Ardinger, R.A. Pagon, S.E. Wallace, L.J.H. Bean, K. Stephens, and A. Amemiya, eds. (Seattle: University of Washington), https://www.ncbi.nlm.nih.gov/books/NBK1182/.

33. Southwood, C.M., Garbern, J., Jiang, W., and Gow, A. (2002). The unfolded protein response modulates disease severity in Pelizaeus-Merzbacher disease. Neuron *36*, 585–596.

34. Gow, A., Gragerov, A., Gard, A., Colman, D.R., and Lazzarini, R.A. (1997). Conservation of topology, but not conformation, of the proteolipid proteins of the myelin sheath. J. Neurosci. *17*, 181–189.

35. Gow, A., Southwood, C.M., and Lazzarini, R.A. (1998). Disrupted proteolipid protein trafficking results in oligodendrocyte apoptosis in an animal model of Pelizaeus-Merzbacher disease. J. Cell Biol. *140*, 925–934.

36. Garbern, J.Y., Yool, D.A., Moore, G.J., Wilds, I.B., Faulk, M.W., Klugmann, M., Nave, K.A., Sistermans, E.A., van der Knaap, M.S., Bird, T.D., et al. (2002). Patients lacking the major CNS myelin protein, proteolipid protein 1, develop length-dependent axonal degeneration in the absence of demyelination and inflammation. Brain *125*, 551–561.

37. Sistermans, E.A., de Coo, R.F., De Wijs, I.J., and Van Oost, B.A. (1998). Duplication of the proteolipid protein gene is the major cause of Pelizaeus-Merzbacher disease. Neurology *50*, 1749–1754.

38. Shetty, R.S., Gallagher, C.S., Chen, Y.T., Hims, M.M., Mull, J., Leyne, M., Pickel, J., Kwok, D., and Slaugenhaupt, S.A. (2011). Specific correction of a splice defect in brain by nutritional supplementation. Hum. Mol. Genet. *20*, 4093–4101.

39. Zhang, Z., Kelemen, O., van Santen, M.A., Yelton, S.M., Wendlandt, A.E., Sviripa, V.M., Bollen, M., Beullens, M., Urlaub, H., Lührmann, R., et al. (2011). Synthesis and characterization of pseudocantharidins, novel phosphatase modulators that promote the inclusion of exon 7 into the SMN (survival of motoneuron) pre-mRNA. J. Biol. Chem. *286*, 10126–10136.

40. Childs-Disney, J.L., Stepniak-Konieczna, E., Tran, T., Yildirim, I., Park, H., Chen, C.Z., Hoskins, J., Southall, N., Marugan, J.J., Patnaik, S., et al. (2013). Induction and reversal of myotonic dystrophy type 1 pre-mRNA splicing defects by small molecules. Nat. Commun. *4*, 2044.

41. Regis, S., Corsolini, F., Grossi, S., Tappino, B., Cooper, D.N., and Filocamo, M. (2013). Restoration of the normal splicing pattern of the PLP1 gene by means of an antisense oligonucleotide directed against an exonic mutation. PLoS ONE *8*, e73633.

42. Havens, M.A., and Hastings, M.L. (2016). Splice-switching antisense oligonucleotides as therapeutic drugs. Nucleic Acids Res. *44*, 6549–6563.

43. Lim, K.R., Maruyama, R., and Yokota, T. (2017). Eteplirsen in the treatment of Duchenne muscular dystrophy. Drug Des. Devel. Ther. *11*, 533–545.

44. Porensky, P.N., and Burghes, A.H. (2013). Antisense oligonucleotides for the treatment of spinal muscular atrophy. Hum. Gene Ther. *24*, 489–498.

45. Passini, M.A., Bu, J., Richards, A.M., Kinnecom, C., Sardi, S.P., Stanek, L.M., Hua, Y., Rigo, F., Matson, J., Hung, G., et al. (2011). Antisense oligonucleotides delivered to the mouse CNS ameliorate symptoms of severe spinal muscular atrophy. Sci. Transl. Med. *3*, 72ra18.

46. Haché, M., Swoboda, K.J., Sethna, N., Farrow-Gillespie, A., Khandji, A., Xia, S., and Bishop, K.M. (2016). Intrathecal Injections in Children With Spinal Muscular Atrophy: Nusinersen Clinical Trial Experience. J. Child Neurol. *31*, 899–906.

47. Chiriboga, C.A., Swoboda, K.J., Darras, B.T., Iannaccone, S.T., Montes, J., De Vivo, D.C., Norris, D.A., Bennett, C.F., and Bishop, K.M. (2016). Results from a phase 1 study of nusinersen (ISIS-SMN(Rx)) in children with spinal muscular atrophy. Neurology *86*, 890–897.

48. Finkel, R.S., Chiriboga, C.A., Vajsar, J., Day, J.W., Montes, J., De Vivo, D.C., Yamashita, M., Rigo, F., Hung, G., Schneider, E., et al. (2016). Treatment of infantile-onset spinal muscular atrophy with nusinersen: a phase 2, open-label, dose-escalation study. Lancet *388*, 3017–3026.

49. Jung, M., Krämer, E., Grzenkowski, M., Tang, K., Blakemore, W., Aguzzi, A., Khazaie, K., Chlichlia, K., von Blankenfeld, G., Kettenmann, H., et al. (1995). Lines of murine oligodendroglial precursor cells immortalized by an activated neu tyrosine kinase show distinct degrees of interaction with axons in vitro and in vivo. Eur. J. Neurosci. *7*, 1245–1265.

50. Pereira, G.B., Dobretsova, A., Hamdan, H., and Wight, P.A. (2011). Expression of myelin genes: comparative analysis of Oli-neu and N20.1 oligodendroglial cell lines. J. Neurosci. Res. *89*, 1070–1078.

51. Wang, E., and Cambi, F. (2009). Heterogeneous nuclear ribonucleoproteins H and F regulate the proteolipid protein/DM20 ratio by recruiting U1 small nuclear ribonucleoprotein through a complex array of G runs. J. Biol. Chem. *284*, 11194–11204.

52. Wang, E., Dimova, N., and Cambi, F. (2007). PLP/DM20 ratio is regulated by hnRNPH and F and a novel G-rich enhancer in oligodendrocytes. Nucleic Acids Res. *35*, 4164–4178.

53. Wang, E., Mueller, W.F., Hertel, K.J., and Cambi, F. (2011). G Run-mediated recognition of proteolipid protein and DM20 5′ splice sites by U1 small nuclear RNA is regulated by context and proximity to the splice site. J. Biol. Chem. *286*, 4059–4071.

54. Summerton, J.E. (2007). Morpholino, siRNA, and S-DNA compared: impact of structure and mechanism of action on off-target effects and sequence specificity. Curr. Top. Med. Chem. *7*, 651–660.

55. Sim, N.L., Kumar, P., Hu, J., Henikoff, S., Schneider, G., and Ng, P.C. (2012). SIFT web server: predicting effects of amino acid substitutions on proteins. Nucleic Acids Res. *40*, W452–457.

56. Adzhubei, I.A., Schmidt, S., Peshkin, L., Ramensky, V.E., Gerasimova, A., Bork, P., Kondrashov, A.S., and Sunyaev, S.R. (2010). A method and server for predicting damaging missense mutations. Nat. Methods *7*, 248–249.

57. Reva, B., Antipin, Y., and Sander, C. (2011). Predicting the functional impact of protein mutations: application to cancer genomics. Nucleic Acids Res. *39*, e118.

58. Schwarz, J.M., Cooper, D.N., Schuelke, M., and Seelow, D. (2014). MutationTaster2: mutation prediction for the deep-sequencing age. Nat. Methods *11*, 361–362.

59. Shihab, H.A., Gough, J., Cooper, D.N., Stenson, P.D., Barker, G.L., Edwards, K.J., Day, I.N., and Gaunt, T.R. (2013). Predicting the functional, molecular, and phenotypic consequences of amino acid substitutions using hidden Markov models. Hum. Mutat. *34*, 57–65.

60. Bachstetter, A.D., Webster, S.J., Van Eldik, L.J., and Cambi, F. (2013). Clinically relevant intronic splicing enhancer mutation in myelin proteolipid protein leads to progressive microglia and astrocyte activation in white and gray matter regions of the brain. J. Neuroinflammation *10*, 146.

61. Edgar, J.M., McCulloch, M.C., Montague, P., Brown, A.M., Thilemann, S., Pratola, L., Gruenenfelder, F.I., Griffiths, I.R., and Nave, K.A. (2010). Demyelination and axonal preservation in a transgenic mouse model of Pelizaeus-Merzbacher disease. EMBO Mol. Med. *2*, 42–50.

62. Medana, I.M., and Esiri, M.M. (2003). Axonal damage: a key predictor of outcome in human CNS diseases. Brain *126*, 515–530.

63. Landel, V., Baranger, K., Virard, I., Loriod, B., Khrestchatisky, M., Rivera, S., Benech, P., and Féron, F. (2014). Temporal gene profiling of the 5XFAD transgenic mouse model highlights the importance of microglial activation in Alzheimer's disease. Mol. Neurodegener. *9*, 33.

64. Clark, K., Sakowski, L., Sperle, K., Banser, L., Landel, C.P., Bessert, D.A., Skoff, R.P., and Hobson, G.M. (2013). Gait abnormalities and progressive myelin degeneration in a new murine model of Pelizaeus-Merzbacher disease with tandem genomic duplication. J. Neurosci. *33*, 11788–11799.

65. Osório, M.J., and Goldman, S.A. (2018). Neurogenetics of Pelizaeus-Merzbacher disease. Handb. Clin. Neurol. *148*, 701–722.

66. Spörkel, O., Uschkureit, T., Büssow, H., and Stoffel, W. (2002). Oligodendrocytes expressing exclusively the DM20 isoform of the proteolipid protein gene: myelination and development. Glia *37*, 19–30.

67. Venkatesh, B., Erdmann, M.V., and Brenner, S. (2001). Molecular synapomorphies resolve evolutionary relationships of extant jawed vertebrates. Proc. Natl. Acad. Sci. USA *98*, 11382–11387.

68. Niks, E.H., and Aartsma-Rus, A. (2017). Exon skipping: a first in class strategy for Duchenne muscular dystrophy. Expert Opin. Biol. Ther. *17*, 225–236.

69. Glascock, J.J., Osman, E.Y., Coady, T.H., Rose, F.F., Shababi, M., and Lorson, C.L. (2011). Delivery of therapeutic agents through intracerebroventricular (ICV) and intravenous (IV) injection in mice. J. Vis. Exp. (56), 2968.

70. R Core Team (2008). R: A language and environment for statistical computing. R Foundation for Statistical Computing, http://www.R-project.org.

71. Nance, M.A., Boyadjiev, S., Pratt, V.M., Taylor, S., Hodes, M.E., and Dlouhy, S.R. (1996). Adult-onset neurodegenerative disorder due to proteolipid protein gene mutation in the mother of a man with Pelizaeus-Merzbacher disease. Neurology *47*, 1333–1335.